Asociación Argentina
de Mecánica Computacional

Mecánica Computacional Vol XXX, págs. 2209-2223 (artículo completo)
Oscar Möller, Javier W. Signorelli, Mario A. Storti (Eds.)
Rosario, Argentina, 1-4 Noviembre 2011

INTERFACE-TRACKING FREE-SURFACE FLOWS IN OPEN DOMAINS

Laura Battaglia[a,b], Mario A. Storti[a] and Jorge D'Elía[a]

[a]*Centro Internacional de Métodos Computacionales en Ingeniería (CIMEC)*
Instituto de Desarrollo Tecnológico para la Industria Química (INTEC)
Universidad Nacional del Litoral - CONICET Güemes 3450, 3000-Santa Fe, Argentina
e-mail: lbattaglia@santafe-conicet.gob.ar, (mstorti,jdelia)@intec.unl.edu.ar
web page: http://www.cimec.org.ar

[b]*Grupo de Investigación en Métodos Numéricos en Ingeniería (GIMNI)*
Universidad Tecnológica Nacional - Facultad Regional Santa Fe
Lavaise 610, 3000-Santa Fe, Argentina

Keywords: fluid mechanics, free surface, arbitrary Lagrangian-Eulerian method, open boundaries.

Abstract. An arbitrary Lagrangian-Eulerian method is used for solving incompressible free-surface flows with the finite element method, assuming that the fluid is viscous and Newtonian. The flow is represented over a domain with a single fluid, where one of the frontiers is a free surface. The computational scheme consists of three main stages: (i) the resolution of the Navier-Stokes equations for the fluid state, with equal order elements for velocity and pressure, stabilized with the streamline-upwind/Petrov-Galerkin and the pressure-stabilizing/Petrov-Galerkin strategies; (ii) the determination of the free surface displacements, as a function of the velocities from the Navier-Stokes stage; (iii) the mesh update procedure, which is performed by a pseudo-elastic problem solved with the free-surface nodal movements as imposed displacements. The main attention here is focused on open domains, where artificial boundaries are proposed in order to bound the numerical problem. The numerical examples consist of free-surface flows with artificial contours, and the results are compared with reference solutions.

1 INTRODUCTION

Free Surface (FS) flows are one of the most typical problems in fluid mechanics, as well as in engineering applications, such as open channel flows (Güler et al., 1999), or sloshing in liquid storage tanks (Papaspyrou et al., 2004; Hernández-Barrios et al., 2007). As a consequence, several numerical methods were developed to predict the FS displacements, as well as the behavior of the liquid beneath or around that particular interface.

Most popular numerical methods for solving FS flows can be grouped in two families: *interface-capturing* methods and *interface-tracking* methods (Shyy et al., 1996). In general, in interface-capturing methods the numerical domain involves the liquid and the gaseous phase, in such a way that the interface is determined in different ways, e.g. with the zero value of a particular function, as in Level Set methods (Osher and Sethian, 1988), or with a fraction of fluid in each element crossed by the interface, as in Volume-of-Fluid methods (Hirt and Nichols, 1981). These methods allow the resolution of problems with interface breaking or folding, with large displacements. The interface-tracking methods are proposed in such a way that the interface, which constitutes a boundary of the numerical domain, is explicitly modeled with certain entities: (i) particles, in the Marker-and-Cell approach (Oishi et al., 2008) or in particle methods (Idelsohn et al., 2004); (ii) nodes, or faces of elements, as in Arbitrary Lagrangian-Eulerian (ALE) methods (Hughes et al., 1981; Huerta and Liu, 1988), where the domain consists of a single fluid phase and its shape changes in time due to the FS displacements.

In the case of infinite, semi-infinite, or large domains, where the FS and the flow are crossed by an artificial boundary which is needed to bound the domain for the numerical analysis, wave reflection problems on artificial contours arise. Then, as a possible solution, *Absorbing* (ABC) or *Non-Reflective* (NRBC) boundary conditions are usually proposed for FS flows (Clément, 1996), either in the inlet or the outlet of the truncated domain. For advective-diffusive problems in general, ABC can be given in a *non-local* or a *local* approach. In the first case, the solutions are usually more accurate; however, these are also more expensive (Storti et al., 2008; Paz et al., 2011). The *local* ABC, more frequent for non-linear fluid dynamic problems, are in general less expensive and easier to implement. Numerous ABC are associated to finite *sacrificial regions*, where the equations involved are modified; this is the case of the so-called absorbing layers, sponges or buffer zones, among others (Colonius, 2004). applications,

In previous works, the ALE approach was employed for solving transient FS flows in closed domains for small and moderate FS displacements (Battaglia et al., 2005, 2006), where the fluid is assumed Newtonian, viscous and incompressible, and is used here for considering open boundary flows. As the domain of analysis is truncated, the waves reflected at the outlet artificial boundaries affect the solution. For recovering an acceptable solution of the problem, the methodology is complemented with the formulation of an Absorbing Layer (AL) that avoids the reflection of the waves on the artificial boundary for FS flows in open domains, considering small amplitude waves. This strategy is based on the eigenvalue decomposition of the advective fluxes, which is easily seen in the shallow-water equations, and is applied later to FS flows.

The programming involved in this work is part of the PETSc-FEM code (PETSc-FEM, 2011), which consists of a series of finite element libraries, developed for parallel computing by using the Message Passing Interface (MPI, 2008) and the Portable Extensible Toolkit for Scientific Computation (PETSc) libraries (Balay et al., 2008).

2 GOVERNING EQUATIONS

The present ALE computing procedure for FS flows consists of solving three alternated instances in each time step, by the Finite Element Method (FEM): (i) the Navier-Stokes (NS) equations, that provide the velocity and the pressure in the fluid domain; (ii) the displacement of the nodes over the FS, determined as a function of the velocities obtained in the first stage; (iii) the new domain shape, deformed as a consequence of the FS displacements, which is performed here through a pseudo-elastic problem, avoiding the remeshing of the domain.

2.1 Navier-Stokes Equations

The NS equations for the ALE approach are (Donea and Huerta, 2003),

$$\rho\left(\partial_t \mathbf{u} + \mathbf{c}\cdot\nabla\mathbf{u} - \mathbf{f}\right) - \nabla\cdot\boldsymbol{\sigma} = 0\ ; \tag{1}$$

$$\nabla\cdot\mathbf{u} = 0\ . \tag{2}$$

over the fluid domain Ω in time $t \in [0, T]$, with flow velocity $\mathbf{u}$, body force $\mathbf{f}$, fluid density ρ, and a given final time T. Furthermore, the fluid stress tensor, $\boldsymbol{\sigma} = \boldsymbol{\sigma}(\mathbf{u}, p)$, is decomposed into an isotropic part, $-p\mathbf{I}$, and a deviatoric one, $\mathbf{T}$,

$$\boldsymbol{\sigma} = -p\mathbf{I} + \mathbf{T}\ ; \tag{3}$$

where p is the pressure, $\mathbf{I}$ is the identity tensor, and $\mathbf{T}$ is

$$\mathbf{T} = 2\mu\boldsymbol{\epsilon}\ ; \tag{4}$$

i.e., it is linearly related to the strain rate $\boldsymbol{\epsilon} = \boldsymbol{\epsilon}(\mathbf{u}) = \frac{1}{2}(\nabla\mathbf{u} + \nabla^T\mathbf{u})$, being μ the fluid dynamic viscosity. The convective velocity $\mathbf{c}$ in Eq. 1 is defined as follows,

$$\mathbf{c} := \mathbf{u} - \hat{\mathbf{u}}; \tag{5}$$

where the velocities $\mathbf{u}$ and $\hat{\mathbf{u}}$ are the fluid and the mesh velocity, respectively.

The boundary conditions for the contours Γ of the fluid domain Ω are typically given by

$$\mathbf{v} = \mathbf{v}_{\mathrm{D}} \qquad \text{on } \Gamma_{\mathrm{D}}; \tag{6}$$

$$\boldsymbol{\sigma}\cdot\mathbf{n} = \mathbf{t} \qquad \text{on } \Gamma_{\mathbf{t}}; \tag{7}$$

with $\Gamma = \Gamma_{\mathrm{D}} \cup \Gamma_{\mathbf{t}}$ and $\Gamma_{\mathrm{D}} \cap \Gamma_{\mathbf{t}} = \emptyset$. Conditions over Γ_{D} are given velocities. generally for solid walls. The interfaces between fluids, constitute the contour $\Gamma_{\mathbf{t}}$; in the case of a FS, the condition consists of the equilibrium between the fluid and the gas stress tensors, $\boldsymbol{\sigma}_l$ and $\boldsymbol{\sigma}_g$, respectively, projected onto the FS normal $\mathbf{n}$,

$$\boldsymbol{\sigma}_l\cdot\mathbf{n} = \boldsymbol{\sigma}_g\cdot\mathbf{n} \qquad \text{on } \Gamma_{\mathrm{FS}}. \tag{8}$$

Since the viscosity and the density of the gas are negligible, then $\mathbf{T}\cdot\mathbf{n} = \mathbf{0}$ and $p = P_{\mathrm{atm}}$ on Γ_{FS}, where P_{atm} is the pressure exerted by the gas over the liquid, considered here as the atmospheric one. Then, the traction forces over the FS are $\mathbf{t} = -P_{\mathrm{atm}}\,\mathbf{n}$.

The Eqs. (1,2) are solved by FEM with the NS module of PETSc-FEM (2011), stabilized with streamline upwind/Petrov-Galerkin (SUPG) (Brooks and Hughes, 1982) and pressure stabilizing/-Petrov-Galerkin (PSPG) (Tezduyar et al., 1992), given the advective character of the equations and the use of linear elements with equal velocity and pressure interpolations.

2.2 Free Surface displacements

The interface displacements are measured over a fixed direction defined for each FS node, represented by a unit vector $\hat{\mathbf{s}}_j$ such that the position $\mathbf{x}_j$ of the node j in time t is (Battaglia et al., 2006)

$$\mathbf{x}_j(t) = \mathbf{x}_{0,j} + \eta_j(t)\, \hat{\mathbf{s}}_j \; ; \tag{9}$$

where $\mathbf{x}_{0,j}$ is the initial position of the node j, and η_j is the scalar coordinate over $\hat{\mathbf{s}}_j$, see Fig. 1. The directions given by $\hat{\mathbf{s}}_j$ are used only for the FS nodal displacements, usually adopted as normal to the FS at rest, while in the rest of the domain the nodal displacements are determined independently of the fluid dynamics.

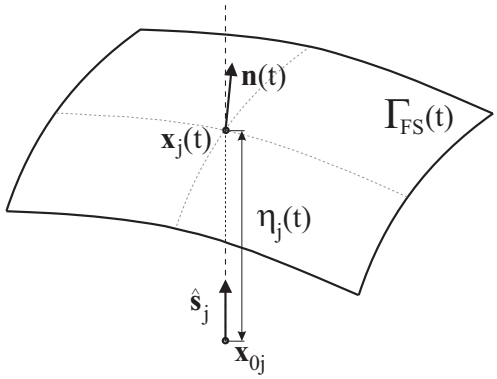

Figure 1: Free surface nodal displacements.

The scalar coordinate η_j is determined from the kinematic FS condition (Pedlosky, 2003),

$$\mathbf{u} \cdot \mathbf{n} = \partial_t \boldsymbol{\eta} \cdot \mathbf{n} \quad \text{over } \Gamma_{\text{FS}}; \tag{10}$$

where

$$\boldsymbol{\eta} = \eta\, \hat{\mathbf{s}} \tag{11}$$

is the FS elevation along $\hat{\mathbf{s}}$, and η is the scalar displacement, see Fig. 1. Replacing in Eq. (10),

$$\partial_t \eta = \frac{\mathbf{u} \cdot \mathbf{n}}{\hat{\mathbf{s}} \cdot \mathbf{n}} \; . \tag{12}$$

As Eq. (12) is a transport equation, the numerical solution of the problem requires numerical stabilization, particularly when the advective terms are dominant. In these cases, a typical SUPG (Brooks and Hughes, 1982) stabilization can be applied in order to avoid numerical instabilities, as in Güler et al. (1999) and Battaglia (2009), among others.

2.3 Mesh movement

The third stage in each time step of the FS flow calculation consists of determining the displacements of the internal nodes. Once the new positions of the FS nodes are known, as described in Sec. 2.2, the input data for the mesh updating procedure is complete.

There are different strategies to take into account the deformation of the domain as a consequence of the FS displacements, considering that such interface constitutes one of the domain contours. Typical methodologies are: (i) remeshing, that is expensive due to the generation of a new mesh and the extrapolation of nodal values for the fluid problem; (ii) algebraic mesh update without mesh topology changes, appropriate for structured meshes with small displacements,

as in classic *spines* methods (Saito and Scriven, 1981); (iii) relocalization of internal nodes by solving an auxiliar problem, e.g. a pseudo-elastic problem (Behr and Abraham, 2002; Rabier and Medale, 2003), or minimizing the elemental distortion of the mesh (López et al., 2007).

Considering the alternative of solving an auxiliary problem, there are two methods available in the PETSC-FEM libraries. For small FS displacements, the pseudo-elastic mesh update is an appropriate choice. The methodology consists of solving an elastic problem over the initial domain Ω, where only Dirichlet conditions are applied. In the case of moderate FS displacement, it is convenient the application of the method proposed in López et al. (2007), that minimizes the distortion of the elements for the deformed domain. Further details about these methodologies can be found in Battaglia (2009); Battaglia et al. (2005).

3 ABSORBING BOUNDARY CONDITIONS

3.1 Absorbing boundary conditions for the shallow water equations

For solving FS flows using the ALE approach, the shallow water (SW) equations can be taken as a reference.

The SW system is

$$\partial_t \mathbf{U} + \partial_x \mathbf{F} = \mathbf{G}; \tag{13}$$

with $\mathbf{U} = [h, u]^T$, $\mathbf{F}(\mathbf{U}) = [hu, \frac{1}{2}u^2 + gh]^T$, $\mathbf{G} = [0, -g\partial_x H^T]$, being h the water height, u the mean horizontal velocity, $\mathbf{F}(\mathbf{U})$ the advective fluxes, g the gravity acceleration, $H = H(x)$ the height of the bottom, and $\mathbf{G}$ the source term given by the variations of the bottom slope.

As it is known, the Jacobian of the flux is

$$A = \frac{\partial \mathbf{F}}{\partial \mathbf{U}} = \begin{bmatrix} u & h \\ g & u \end{bmatrix}; \tag{14}$$

and the corresponding eigenvalue decomposition is

$$A = \mathbf{V}\mathbf{\Lambda}\mathbf{V}^{-1}; \tag{15}$$

where

$$\mathbf{\Lambda} = \begin{bmatrix} u+c & 0 \\ 0 & u-c \end{bmatrix}; \qquad \mathbf{V} = \begin{bmatrix} h & h \\ c & -c \end{bmatrix}; \qquad \mathbf{W} = \mathbf{V}^{-1} = \frac{1}{2}\begin{bmatrix} 1/h & 1/c \\ 1/h & -1/c \end{bmatrix}; \tag{16}$$

and $c = \sqrt{gh}$.

When the flow is subcritic at the outlet, there is one incoming characteristic with velocity $u - c$. By summing an AL term from to the SW equations, Eq. (13), with $\mathbf{U}_{\text{ref}} = [h_0, u_0]^T$, the modified system is

$$\partial_t \mathbf{U} + \partial_x \mathbf{F} + \mathrm{K}\ \mathbf{H}\ (\mathbf{U} - \mathbf{U}_{\text{ref}}) = \mathbf{G}. \tag{17}$$

Then, with $c_0 = \sqrt{gh_0}$,

$$\mathbf{H} = \mathbf{V}\begin{bmatrix} 0 & 0 \\ 0 & u_0 - c_0 \end{bmatrix}\mathbf{W} = (u_0 - c_0)\begin{bmatrix} 1 & -h_0/c_0 \\ -c_0/h_0 & 1 \end{bmatrix}. \tag{18}$$

By writing all the terms, the modified SW equations are as follows,

$$\partial_t h + \partial_x(uh) + K\ h_0\ (u_0 - c_0)\left\{\frac{h - h_0}{h_0} - \frac{u - u_0}{u_0}\right\} = 0; \tag{19}$$

$$\partial_t u + \partial_x(1/2u^2 + gh) + K\ c_0\ (u_0 - c_0)\left\{\frac{h - h_0}{h_0} - \frac{u - u_0}{u_0}\right\} = 0. \tag{20}$$

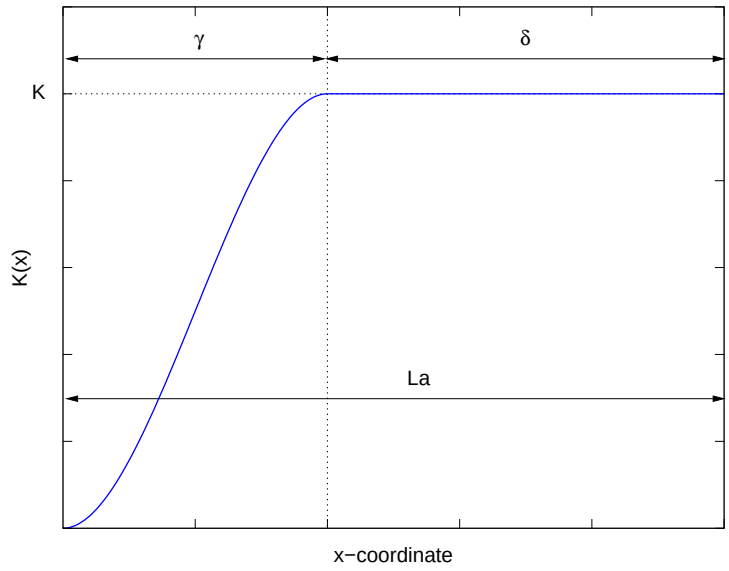

Figure 2: Variation of the penalty parameter K along the absorbing layer of length L_a

.

3.2 Absorbing boundary conditions for FS solved by an ALE strategy

Taking as a reference the concepts from Sec. 3.1, the aim is implementing the absorbing terms of the modified SW equations, Eqs. (19,20), in the ALE-NS equations used for solving FS flows.

Regarding the reference parameters to be replaced, some analogies should be made. First, the horizontal velocity u in SW is an average in height of the velocity; then, for the ALE-NS approach, and considering that near the outlet the wave perturbations are negligible, u can be replaced by the average horizontal flow velocity. Regarding u_0, and assuming that the mean conditions are steady, it can be adopted in an analogous fashion as u; furthermore, it is usually an input data for the computation.

With respect to the mean height, the reference value h_0 will be given, while h has to be obtained from the NS model available information. On the one hand, considering the wave expression from the potential theory,

$$\phi\,(x,y,z) = \tilde{A}\ \exp\left[i(kx-\tilde{\omega}t)\right]\frac{\cosh\,(kz)}{\cosh\,(kh_0)}; \tag{21}$$

being ϕ the velocity potential, k the wave number, $\tilde{A}$ the wave amplitude and $\tilde{\omega}$ the angular frequency, with $z=0$ at the bottom and h_0 the mean height of the water. On the other hand, the Bernoulli equation can provide a relation of the wave shape with the pressure,

$$\frac{p}{\rho}+gz+\partial_t\phi+\frac{1}{2}u^2=\frac{p_{\text{atm}}}{\rho}+gz_0+\frac{1}{2}u_\infty^2=\text{constant}. \tag{22}$$

For small amplitude waves, the quadratic velocity terms can be neglected; re-arranging and introducing $\partial_t\phi$ from Eq. (21), and considering that for small amplitude waves the depth factor is one,

$$\frac{p-p_{\text{atm}}}{\rho}+g(z-z_0)=i\tilde{\omega}\tilde{A}\ \exp\left[i(kx-\tilde{\omega}t)\right]. \tag{23}$$

Over the FS is $p = p_{\rm atm}$; then, the elevation η is

$$\eta = h - h_0 = \frac{i\tilde{\omega}\tilde{A}}{g}\ \exp\left[i(kx - \tilde{\omega}t)\right]. \tag{24}$$

Expressions from Eqs. (23) and (23) are similar, and allows establishing the following approximation,

$$\frac{p - p_{\rm atm}}{\rho\, g} + (z - z_0) \approx \eta = h - h_0. \tag{25}$$

Finally, left hand side of Eq. (25) can be used for replacing $h - h_0$ in the AL term for the NS equations in FS fluid flows.

It is known that the transition from the regular equations, Eqs. (1,2), to the modified ones, i.e. by introducing the term $\mathrm{K}\mathbf{H}(\mathbf{U} - \mathbf{U}_{\rm ref})$, should be smooth for avoiding wave reflections in the transition section (Clément, 1996). Then, the penalization parameter is chosen for this approach as a function of the position in x-coordinates, i.e. $\mathrm{K} = \mathrm{K}(x)$, such that the AL is divided in two regions, see Fig. 2. In the first region, γ, the penalty parameter grows from 0 to the maximum value K following a cubic polinomial variation. In the other region, named δ, the value of K is kept constant.

4 NUMERICAL EXAMPLE

4.1 Problem description

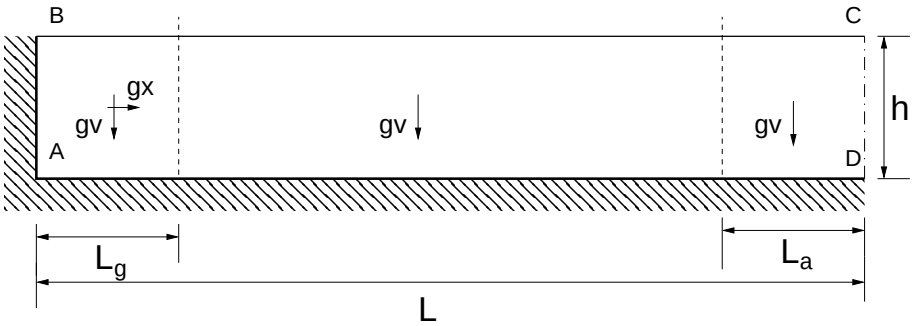

Figure 3: Numerical example. Domain geometry.

The numerical example consists of a rectangle of length $L = 20$ m and water depth of $h = 1$ m, sketched in Fig. 3, where waves are generated in the left part of the domain, over a length of $L_g = 1.9365$ m. Slip boundary conditions are given for side AB of the domain, as well as for the bottom AD, i.e. $\mathbf{u} \cdot \hat{\mathbf{n}} = 0$, with $\hat{\mathbf{n}}$ the unit vector perpendicular to the walls. The free surface is defined by the contour BC, with $P_{\rm atm} = 0$, and side CD constitutes the artificial boundary, also with a slip condition applied, $\mathbf{u} \cdot \hat{\mathbf{n}} = 0$.

The fluid is considered Newtonian and incompressible, with kinematic viscosity $\nu = 1 \times 10^{-5}$ m^{2}s^{-1} and density $\rho = 1$ kg m^{-3}. The gravity acceleration in the vertical direction is $g_v = 1$ m s^{-2}, and for the wave generation region, the horizontal gravity component g_x is given by the following expression,

$$g_x = A\ g_v\ \sin(\omega t); \tag{26}$$

where $A = 0.02$ is a given amplitude, $\omega = 2\pi$ is the imposed acceleration frequency and t is the time. The wave propagation velocity is $c = \sqrt{g_v\, h} = 1$ m s^{-1}, and the wavelength is $\lambda = 3.873$ m.

4.2 Numerical solutions

The numerical simulation was performed over a FE regular mesh with quadrangular elements of side length $h_e = 0.10$ m. The analysis was performed for 4000 time steps of $\Delta t = 0.025$ s.

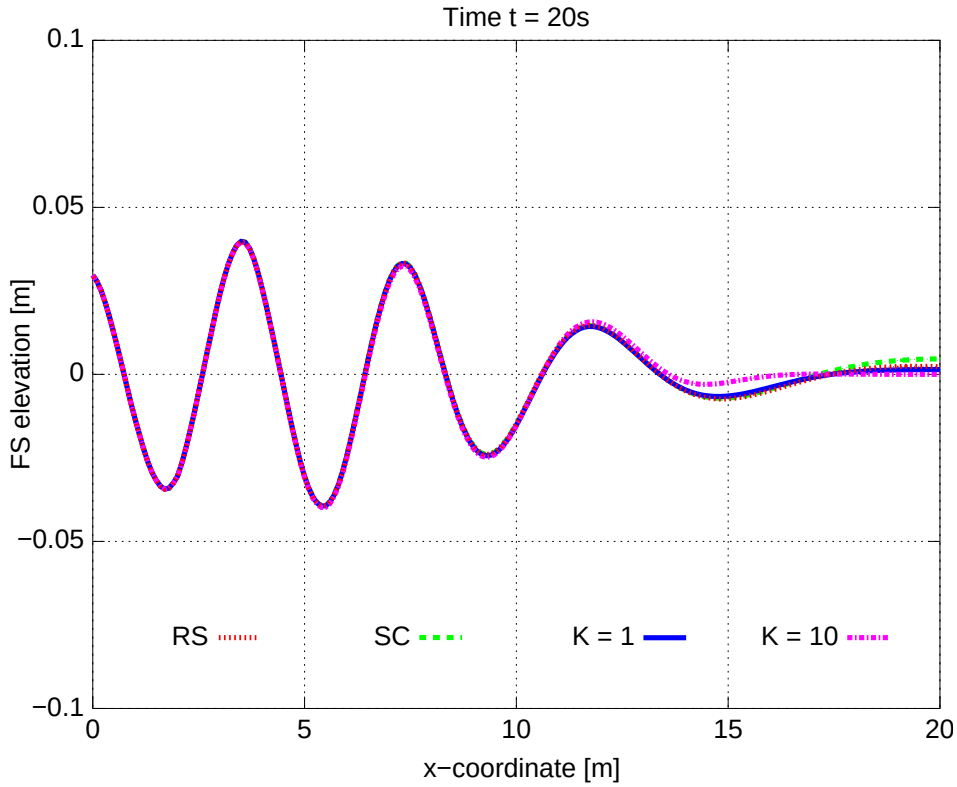

Figure 4: Numerical example. Free surface elevation for the reference solution (RS), the solution in the short domain with slip condition at the outlet (SC), and the last two solved with absorbing boundary conditions (ABC), in time $t = 20$ s.

Three different solutions were proposed:

1. Reference Solution (RS) with an extended domain $L_T = 3L$; the results are taken as a reference due to the lack of reflected waves for the analyzed time and length ranges;

2. Slip Condition (SC) with the regular domain of length L applied over the right boundary for the regular domain of length L, which shows spurious wave reflections;

3. Absorbing Boundary Condition (ABC) cases, where the proposed methodology was applied over the last part of the domain over a length $L_a = 7.75$ m, for two penalization parameter K values, and a total domain length of L.

The Figs. 4 to 7 show the FS elevation in different times of the simulations, as a function of the x-coordinates. The curves plotted represent the RS, the SC and two ABC cases with transition length $\gamma = \lambda = 3.873$ m for the absorbing layer, total absorbing layer of $L_a = 2\lambda = 7.75$ m, and penalization values $\mathrm{K} = 1$ and $\mathrm{K} = 10$.

In Fig. 4, there are no significant differences among the four curves represented, due to that the wave train arrives to the right boundary at that time, $t = 20$ s.

Figure 5, for $t = 40$ s, shows the decrease in the amplitude for the ABC solutions approximately after $x \approx 14$ m, being the most importan the one with $\mathrm{K} = 10$. On the one side, from

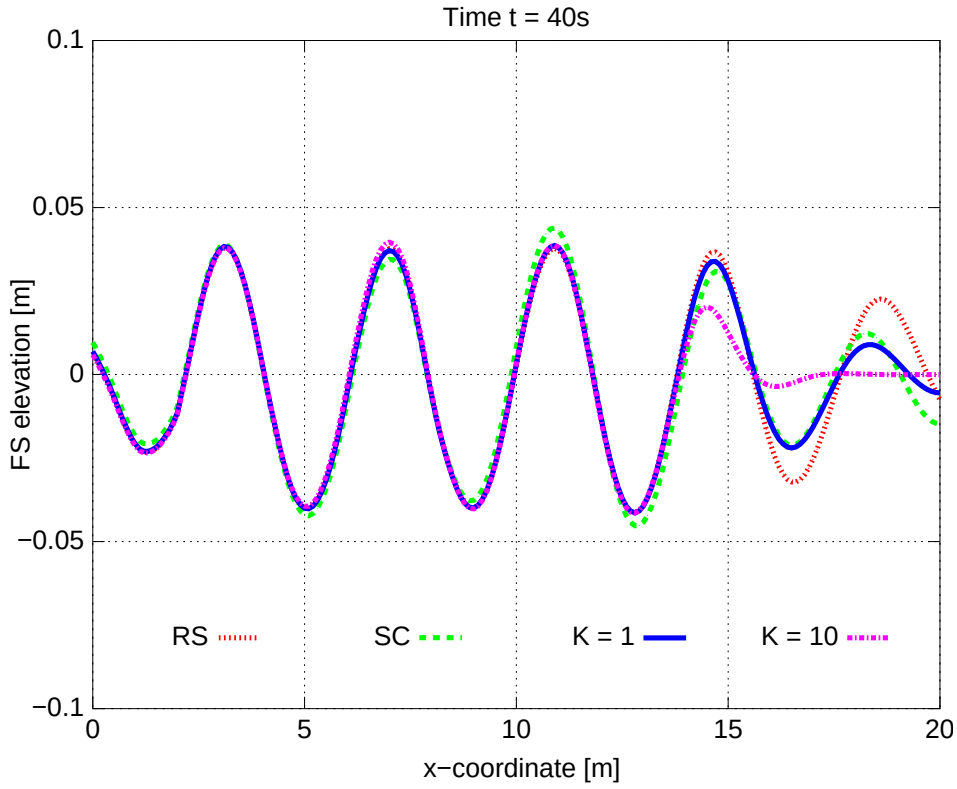

Figure 5: Numerical example. Free surface elevation for the reference solution (RS), the solution in the short domain with slip condition at the outlet (SC), and the last two solved with absorbing boundary conditions (ABC), in time $t = 40$ s.

the same figure, the curves ABC and RS show small differences among them over most of the domain. By the other side, the curve SC shows a behaviour different from the curve RS, due to the wave reflections over the right boundary.

For time $t = 60$ s, the ABC solution with $\mathrm{K} = 10$ keeps showing the decrease in the amplitude, see Fig. 6, while the SC solution exhibits an important increment of the amplitude, due to the waves reflected. The ABC solution with $\mathrm{K} = 1$ shows also a small increment of the amplitude with respect to RS.

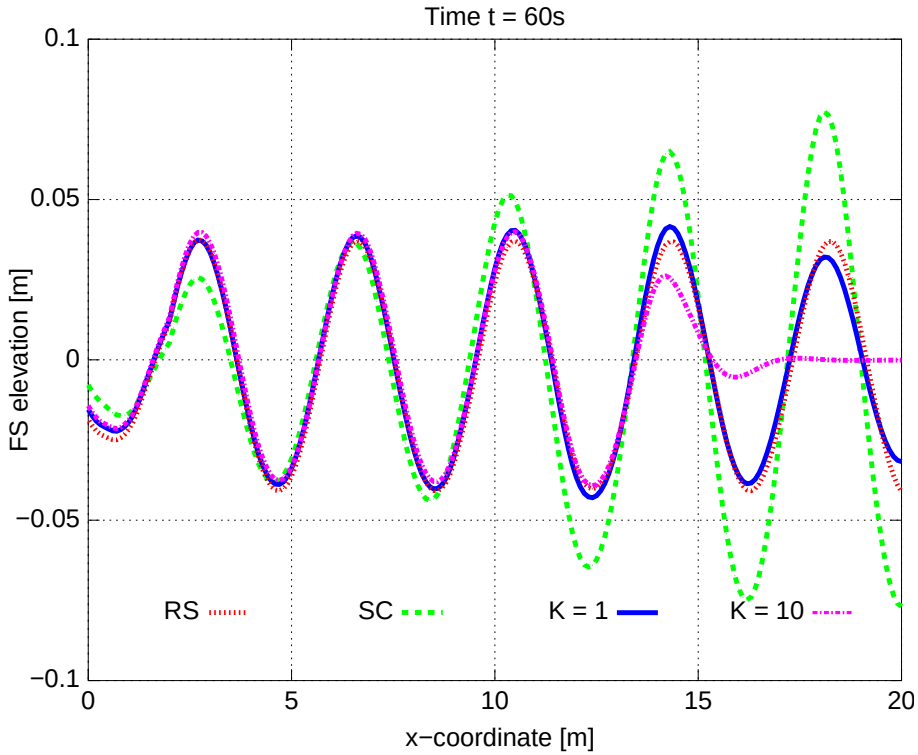

Figure 6: Numerical example. Free surface elevation for the reference solution (RS), the solution in the short domain with slip condition at the outlet (SC), and the last two solved with absorbing boundary conditions (ABC), in time $t = 60$ s.

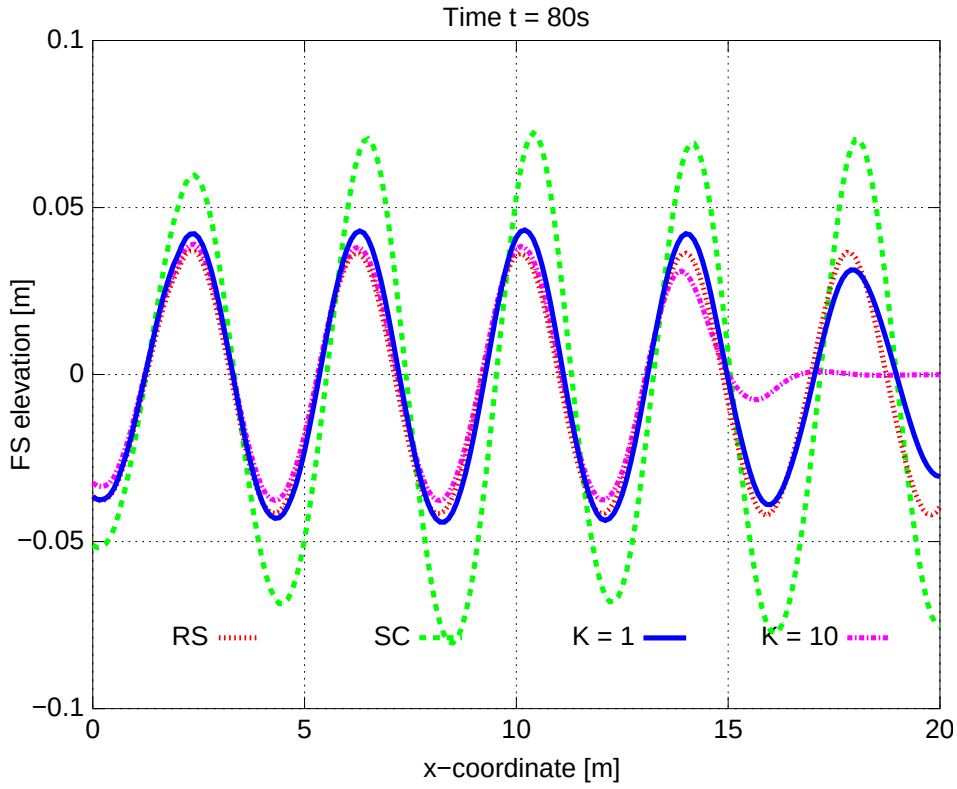

Figure 7: Numerical example. Free surface elevation for the reference solution (RS), the solution in the short domain with slip condition at the outlet (SC), and the last two solved with absorbing boundary conditions (ABC), in time $t = 80$ s.

Finally, the curves appreciated in Fig 7 for $t = 80$ s repeat somehow the picture described for time $t = 60$ s: the non-uniform increment of the wave amplitude for SC, and a minor amplitude increment for ABC with $\mathrm{K} = 1$. The ABC curve with $\mathrm{K} = 10$ fits better the RS curve, although the amplitude of the former is a little lower than expected.

Other indicator to be analized is the maximum wave amplitude measured in each time step along the analysis, that is represented in Fig. 8. On the one hand, the RS results show along the analysis an almost uniform wave amplitude, with small quasi-periodic decayment due to the viscous effects, at least over length L, taking into account that this solution was obtained for an extended domain. On the other hand, the SC solution presents an increment and a strong variation in the maximum wave amplitude for each time step, which is due to the superposition of the right-travelling waves and the reflected ones. At last, the solution ABC shows a smooth amplitude variation, very similar to the one registered in RS. Then, the use of ABCs over the oulet region of length $L_a = 2\lambda$ with a transition of length λ, as described in Sec. 3.2, provided suitable results for the semi-infinite problem of travelling waves using a finite extension domain.

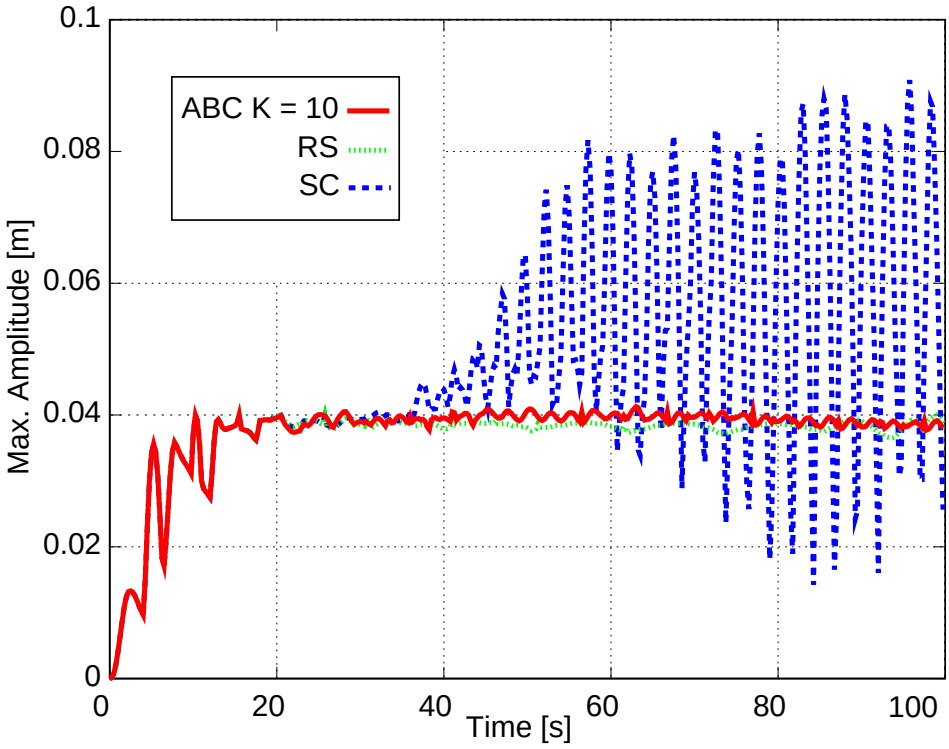

Figure 8: Numerical example. Maximum amplitude in each time step for the reference solution (RS), the solution in the short domain with slip condition at the outlet (SC), and the last one solved with absorbing boundary conditions (ABC) with a penalization of $\mathrm{K} = 10$.

5 CONCLUSIONS

A linear absorbing boundary conditions suitable for free surface flows with open domains, solved in an ALE framework, was introduced. The methodology is based on a proposal for the resolution of the shallow water equations for infinite domains, described in Sec. 3.1, and is implemented so far for flows without a mean flow current. The application example from Sec. 4.1 shows that the absorbing condition was able to reduce the incoming spurious reflected waves over the artificial boundary of a two-dimensional problem, and the influence of the penalization parameter K on the results. Further work will be focused on (i) establishing appropriate values for K and for the absorbing/transition lengths, called here L_a, and (ii) the generalization of the method for two- and three-dimensional free surface flows with mean current and artificial boundaries.

Acknowledgments This work has received financial support from Consejo Nacional de Investigaciones Científicas y Técnicas (CONICET, Argentina), Universidad Nacional del Litoral (UNL, Argentina, grants CAI+D 65-334/2009, CAI+D III-4-2/2009) and Agencia Nacional de Promoción Científica y Tecnológica (ANPCyT, Argentina, grants PICT 0270/2008, PICT 01141/2007, PICT 2492/2010), and was partially performed with the *Free Software Foundation GNU-Project* resources as GNU/Linux OS and GNU/Octave, as well as other Open Source resources as PETSc, MPICH, Paraview, LaTeX and JabRef.

REFERENCES

Balay S., Buschelman K., Eijkhout V., Gropp W., Kaushik D., Knepley M., McInnes L., Smith B., and Zhang H. PETSc Users Manual. ANL 95/11 - Revision 3.0.0, Argonne National Laboratory, 2008.

Battaglia L. *Stabilized Finite Elements for Free Surface Flows: Tracking and Capturing of the Interface*. Ph.D. thesis, Facultad de Ingeniería y Ciencias Hídricas, Universidad Nacional del Litoral, Santa Fe, Argentina, 2009.

Battaglia L., D' Elía J., Storti M.A., and Nigro N.M. Free-surface flows in a multi-physics programming paradigm. In A. Larreteguy, editor, *Mecánica Computacional*, volume XXIV, pages 105–116. 2005.

Battaglia L., D' Elía J., Storti M.A., and Nigro N.M. Numerical simulation of transient free surface flows using a moving mesh technique. *ASME Journal of Applied Mechanics*, 73(6):1017–1025, 2006. doi:10.1115/1.2198246.

Behr M. and Abraham F. Free surface flow simulations in the presence of inclined walls. *Computer Methods in Applied Mechanics and Engineering*, 191(47-48):5467–5483, 2002.

Brooks A. and Hughes T.J.R. Streamline upwind/Petrov-Galerkin formulations for convection dominated flows with particular emphasis on the incompressible Navier-Stokes equations. *Computer Methods in Applied Mechanics Engineering*, 32(1-3):199–259, 1982. doi:10.1016/0045-7825(82)90071-8.

Clément A. Coupling of two absorbing boundary conditions for 2d time-domain simulations of free surface gravity waves. *Journal of Computational Physics*, 126(1):139 – 151, 1996. ISSN 0021-9991. doi:10.1006/jcph.1996.0126.

Colonius T. Modeling artificial boundary conditions for compressible flow. *Annual Review of Fluid Mechanics*, 36:315–345, 2004. doi:10.1146/annurev.fluid.36.050802.121930.

Donea J. and Huerta A. *Finite Element Methods for Flow Problems*. John Wiley & Sons, 2003.

Güler I., Behr M., and Tezduyar T.E. Parallel finite element computation of free-surface flows. *Computational Mechanics*, 23(2):117–123, 1999. doi:10.1007/s004660050391.

Hernández-Barrios H., Heredia-Zavoni E., and Aldama-Rodríguez A.A. Nonlinear sloshing response of cylindrical tanks subjected to earthquake ground motion. *Engineering Structures*, 29(12):3364 – 3376, 2007. ISSN 0141-0296. doi:10.1016/j.engstruct.2007.08.023.

Hirt C.W. and Nichols B.D. Volume of fluid (VOF) method for the dynamics of free boundaries. *Journal of Computational Physics*, 39(1):201–225, 1981. doi:10.1016/0021-9991(81)90145-5.

Huerta A. and Liu W.K. Viscous flow with large free surface motion. *Computer Methods in Applied Mechanics and Engineering*, 69:277–324, 1988.

Hughes T.J.R., Liu W.K., and Zimmermann T.K. Lagrangian-Eulerian finite element formulation for incompressible viscous flows. *Computer Methods in Applied Mechanics and Engineering*, 29(3):329–349, 1981. doi:10.1016/0045-7825(81)90049-9.

Idelsohn S.R., Oñate E., and Del Pin F. The Particle Finite Element Method: a powerful tool to solve incompressibleflows with free-surfaces and breaking waves. *International Journal for Numerical Methods in Engineering*, 61(7):964–984, 2004.

López E.J., Nigro N.M., Storti M.A., and Toth J.A. A minimal element distortion strategy for computational mesh dynamics. *International Journal for Numerical Methods in Engineering*, 69(9):1898–1929, 2007.

MPI. Message Passing Interface. http://www.mpi-forum.org/docs/docs.html, 2008.

Oishi C.M., Tome M.F., Cuminato J.A., and McKee S. An implicit technique for solving 3D low Reynolds number moving free surface flows. *Journal of Computational Physics*, 227(16):7446–7468, 2008. doi:10.1016/j.jcp.2008.04.017.

Osher S. and Sethian J.A. Fronts propagating with curvature-dependent speed: Algorithms based on Hamilton-Jacobi formulations. *Journal of Computational Physics*, 79(1):12–49, 1988. doi:10.1016/0021-9991(88)90002-2.

Papaspyrou S., Valougeorgis D., and Karamanos S.A. Sloshing effects in half-full horizontal cylindrical vessels under longitudinal excitation. *ASME-Journal of Applied Mechanics*, 71(2):255–265, 2004. doi:10.1115/1.1668165.

Paz R.R., Storti M.A., and Garelli L. Local absorbent boundary condition for non-linear hyperbolic problems with unknown Riemann invariants. *Computers & Fluids*, 40(1):52 – 67, 2011. ISSN 0045-7930. doi:10.1016/j.compfluid.2010.08.001.

Pedlosky J. *Waves in the ocean and atmosphere. Introduction to wave dynamics*. Springer, 2003.

PETSc-FEM. A general purpose, parallel, multi-physics FEM program. 2011. GNU General Public License (GPL).

Rabier S. and Medale M. Computation of free surface flows with a projection FEM in a moving mesh framework. *Computer Methods in Applied Mechanics and Engineering*, 192(41-42):4703–4721, 2003. doi:10.1016/S0045-7825(03)00456-0.

Saito H. and Scriven L.E. Study of coating flow by the finite element method. *Journal of Computational Physics*, 42(1):53–76, 1981. doi:10.1016/0021-9991(81)90232-1.

Shyy W., Udaykumar H.S., Rao M.M., and Smith R.W. *Computational Fluid Dynamics with Moving Boundaries*. Taylor and Francis, 1996.

Storti M.A., Nigro N.M., Paz R.R., and Dalcín L.D. Dynamic boundary conditions in computational fluid dynamics. *Computer Methods in Applied Mechanics Engineering*, 197(13–16):1219–1232, 2008. doi:10.1016/j.cma.2007.10.014. Elsevier, Amsterdam, The Netherlands.

Tezduyar T.E., Mittal S., Ray S.E., and Shih R. Incompressible flow computations with stabilized bilinear and linear-equal-order interpolation velocity-pressure elements. *Computer Methods in Applied Mechanics and Engineering*, 95(2):221–242, 1992. doi: 10.1016/0045-7825(92)90141-6.